

SUPPLEMENTARY INFORMATION

**Modulation of the elasticity of single crystal, 1-D metal dimethylglyoximate complexes via solid solution effect**

Akira Sugimoto,<sup>a</sup> Sotaro Kusumoto,<sup>b</sup> Manabu Nakaya,<sup>c</sup> Yoshihiro Sekine,<sup>ad</sup> Leonard F. Lindoy,<sup>e</sup> and Shinya Hayami <sup>\*afg</sup>

<sup>a</sup> Department of Chemistry, Graduate School of Science and Technology, Kumamoto University, 2-39-1 Kurokami, Chuo-ku, Kumamoto 860-8555, Japan.

<sup>b</sup> Department of Material and Life Chemistry, Faculty of Engineering, Kanagawa University, 3-27-1 Rokkakubashi, Kanagawa-ku, Yokohama 221-8686, Japan.

<sup>c</sup> Department of Chemistry, Faculty of Science, Josai University, 1-1 Keyakidai, Sakado, Saitama 350-0295, Japan

<sup>d</sup> Priority Organization for Innovation and Excellence, Kumamoto University, 2-39-1 Kurokami, Chuo-ku, Kumamoto 860-8555, Japan

<sup>e</sup> School of Chemistry F11, The University of Sydney, Sydney, New South Wales, 2006, Australia

<sup>f</sup> Institute of Industrial Nanomaterials (IINa), Kumamoto University, 2-39-1 Kurokami, Chuo-ku, Kumamoto 860-8555, Japan

<sup>g</sup> International Research Center for Agricultural and Environmental Biology (IRCAEB), Kumamoto University, 2-39-1 Kurokami, Chuo-ku, Kumamoto 860-8555, Japan

Corresponding author: S. Hayami  
E-mail: hayami@kumamoto-u.ac.jp

## Syntheses

All reagents and solvents were purchased from Tokyo Kasei Co. and Wako Pure Chemical Industries and used without further purification. [M(HDMG)<sub>2</sub>] (M = Ni(**1**), Pd(**2**), Pt(**3**)) complexes were prepared according to the literature.<sup>1–3</sup>

[Ni(HDMG)<sub>2</sub>] (**1**): An EtOH solution (10 mL) of H<sub>2</sub>DMG (= N,N'-dihydroxy-2,3-butanediimine; 580 mg, 5 mmol) was added to a stirred EtOH solution (10 mL) of Ni(OAc)<sub>2</sub>·4H<sub>2</sub>O (622 mg, 2.5 mmol), then the solution was refluxed for 1 h. The red precipitate was collected by filtration, washed with EtOH and dried *in vacuo*. The precipitate was dissolved in boiling DMF (N,N-dimethylmethanamide) and the solution was allowed to cool slowly over one day to yield red needle-shaped single crystals of **1**. Anal. Calc.: C, 33.26; H, 4.88; N, 19.39. Found: C, 33.27; H, 5.21; N, 19.55.

[Pd(HDMG)<sub>2</sub>] (**2**): A hot EtOH solution (30 mL) of H<sub>2</sub>DMG (348 mg, 3 mmol) was added to a hot stirred aqueous solution (30 mL) of PdCl<sub>2</sub> (266 mg, 1.5 mmol), then the solution was refluxed for 2 h. The yellow precipitate that formed was collected by filtration, washed with H<sub>2</sub>O then EtOH and dried *in vacuo*. The precipitate was dissolved in boiling DMF and the solution was allowed to cool slowly over one day to yield yellow needle-shaped single crystals of **2**. Anal. Calc.: C, 28.54; H, 4.19; N, 16.64. Found: C, 28.62; H, 4.58; N, 16.75.

[Pt(HDMG)<sub>2</sub>] (**3**): An EtOH solution (10 mL) of H<sub>2</sub>DMG (174 mg, 1.5 mmol) was added to a stirred 1% HCl(aq) solution (10 mL) of K<sub>2</sub>[PtCl<sub>4</sub>] (200 mg, 0.5 mmol). The resulting solution was heated at reflux for 3 h. The violet precipitate that formed was collected by filtration, washed with H<sub>2</sub>O then EtOH, and dried *in vacuo*. The precipitate was dissolved in boiling DMF and the solution was allowed to cool slowly over one day to yield dark red needle-shaped single crystals of **3**. Anal. Calc.: C, 22.59; H, 3.22; N, 13.17. Found: C, 22.68; H, 3.74; N, 13.28.

Binary solid solution single crystals of **4** (Ni/Pd), **5** (Ni/Pt) or **6** (Pd/Pt) were obtained by dissolving the required two metal complexes chosen from **1**, **2** or **3** (each at 0.05 mmol) in boiling DMF (50 mL). In each case the resulting solution was filtered while hot and the filtrates were allowed to cool over 1 h. The solid solution microcrystals that formed were collected by filtration. The respective products were then redissolved in boiling DMF (50 mL) and the solutions were allowed to cool slowly over one day to yield needle-shaped single crystals of the solid solutions **4**, **5** and **6**. ICP-OES analyses were carried out to determine the ratio of metal ions present in each of these products.

## Physical measurements

Elemental analyses were carried out using a J-SCIENCE LAB JM10 analyser at the Instrumental Analysis Centre of Kumamoto University. ICP-OES analyses were carried out using a Seiko Instruments Inc. SPS7800 Plasma Spectrometer. Single crystal X-ray diffraction data for **1–6** were recorded on a Rigaku FR-E+ diffractometer equipped with a HyPix-6000 area detector, using multi-layer mirror monochromated Mo-K $\alpha$  radiation ( $\lambda = 0.71073 \text{ \AA}$ ). Data integration and reduction were undertaken with CrysAlisPro. Using OLEX crystallographic software package, the structure was solved with the SHELXT structure solution program using Direct Methods and refined with the SHELXL refinement package using least squares minimization. Hydrogen atoms were included in idealized positions and refined using a riding model. Crystallographic data is summarised in Table S1, S2. Powder X-ray diffraction data (PXRD) were collected on a Rigaku MiniFlex II ultra (30 kV/15 mA) X-ray diffractometer using Cu K $\alpha$  radiation ( $\lambda = 1.5406 \text{ \AA}$ ) in the  $2\theta$  range of  $5^\circ$ – $30^\circ$  with a step width of  $0.5^\circ$ . Elastic bending for calculation of elastic strain ( $\varepsilon$ ) was carried out using an Olympus BX 53, and the recordings were taken and processed using the Leica Application Suite ver. 3.2.0. Each measurement was conducted using three different crystals and the quoted  $\varepsilon$  values are the averaged values from the three measurements.<sup>4</sup>

## Supplementary data

Table S1. Crystallographic data for 1–3.

Compound	1	2	3
formula	C <sub>8</sub> H <sub>14</sub> N <sub>4</sub> NiO <sub>4</sub>	C <sub>8</sub> H <sub>14</sub> N <sub>4</sub> O <sub>4</sub> Pd	C <sub>8</sub> H <sub>14</sub> N <sub>4</sub> O <sub>4</sub> Pt
formula weight	288.94	336.63	425.32
crystal system	Orthorhombic	Orthorhombic	Orthorhombic
space group	<i>lbam</i>	<i>lbam</i>	<i>lbam</i>
<i>a</i> / Å	16.210(2)	16.3415(10)	16.2744(11)
<i>b</i> / Å	10.5207(16)	10.6382(6)	10.6919(7)
<i>c</i> / Å	6.3360(9)	6.3897(4)	6.3727(4)
$\alpha$ / °	90	90	90
$\beta$ / °	90	90	90
$\gamma$ / °	90	90	90
<i>V</i> / Å <sup>3</sup>	1080.54	1110.81	1108.88
<i>Z</i>	4	4	4
<i>T</i> / K	123	123	123
<i>R</i> <sub>1</sub> [ <i>I</i> > 2 $\sigma$ ( <i>I</i> )]	0.0480	0.0207	0.0170
<i>wR</i> <sub>2</sub> [ <i>I</i> > 2 $\sigma$ ( <i>I</i> )]	0.1277	0.0592	0.0439
<i>R</i> <sub>1</sub> (all data)	0.0566	0.0215	0.0215
<i>wR</i> <sub>2</sub> (all data)	0.1333	0.0600	0.0456
CCDC	2149607	2149869	2149870

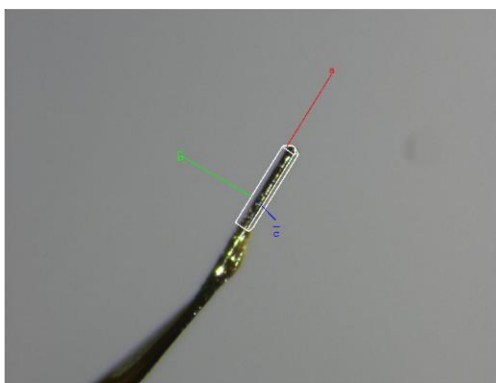
Table S2. Crystallographic data for 4–6.

Compound	4	5	6
formula	C <sub>8</sub> H <sub>14</sub> N <sub>4</sub> O <sub>4</sub> Ni <sub>0.599</sub> Pd <sub>0.401</sub>	C <sub>8</sub> H <sub>14</sub> N <sub>4</sub> O <sub>4</sub> Ni <sub>0.551</sub> Pt <sub>0.449</sub>	C <sub>8</sub> H <sub>14</sub> N <sub>4</sub> O <sub>4</sub> Pd <sub>0.507</sub> Pt <sub>0.493</sub>
formula weight	308.14	350.99	380.98
crystal system	Orthorhombic	Orthorhombic	Orthorhombic
space group	<i>lbam</i>	<i>lbam</i>	<i>lbam</i>
<i>a</i> / Å	10.5483(7)	10.5843(8)	16.3923(12)
<i>b</i> / Å	16.3439(10)	16.3239(11)	10.6456(7)
<i>c</i> / Å	6.3648(4)	6.3513(4)	6.3980(4)
$\alpha$ / °	90	90	90
$\beta$ / °	90	90	90
$\gamma$ / °	90	90	90
<i>V</i> / Å <sup>3</sup>	1097.29(12)	1097.36(13)	1116.49(13)
<i>Z</i>	4	4	4
<i>T</i> / K	123	123	123
<i>R</i> <sub>1</sub> [ <i>I</i> > 2 $\sigma$ ( <i>I</i> )]	0.0219	0.0229	0.0214
<i>wR</i> <sub>2</sub> [ <i>I</i> > 2 $\sigma$ ( <i>I</i> )]	0.0538	0.0542	0.0572
<i>R</i> <sub>1</sub> (all data)	0.0251	0.0303	0.0277
<i>wR</i> <sub>2</sub> (all data)	0.0554	0.0561	0.0605
CCDC	2149871	2149872	2149873

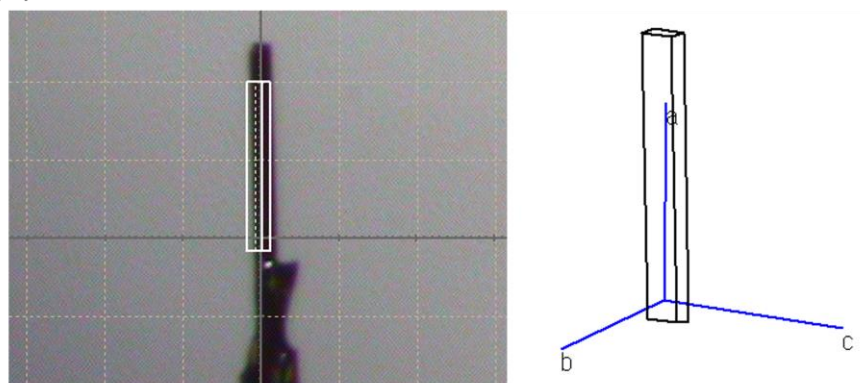
**Table S3.** Metal-to-metal distance in the interchain direction.

	1	2	3	4	5	6
Metal-to-metal distance (Å) for <i>b</i> -axis	10.5207	10.6382	10.6914	10.5483	10.5843	10.6456

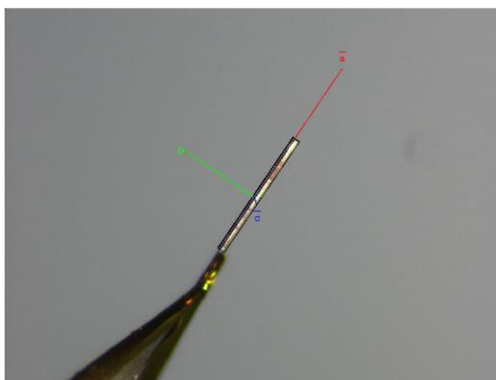
(a)



(b)



(c)

**Fig. S1.** Face indexing of (a) 1, (b) 2, (c) 3.

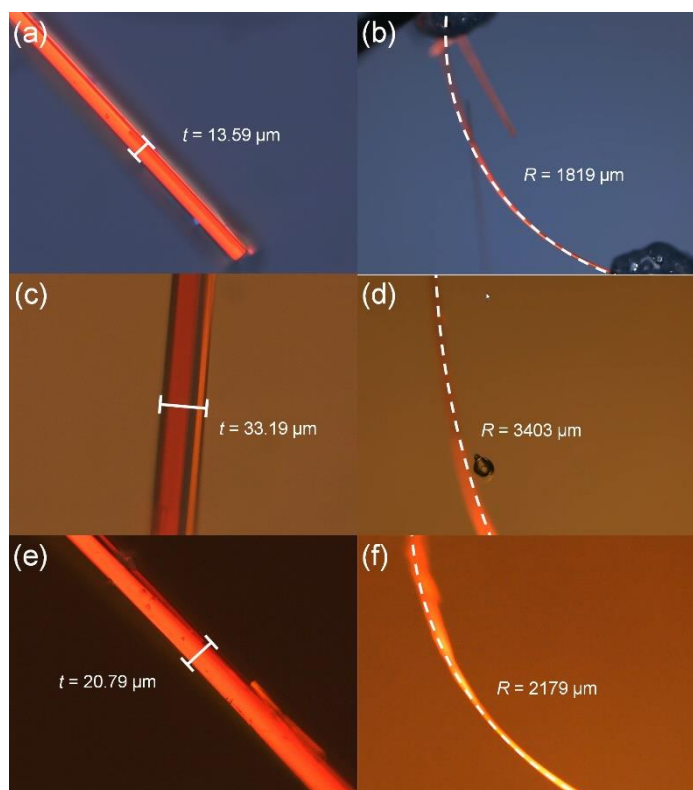


**Fig. S2.** Strain measurement for crystals of **1**. The maximum elastic strain is calculated using the thickness ( $t$ ) of the crystals (a, c, and e) and the radius ( $R$ ) of the bending loop at the critical state (b, d, and e).

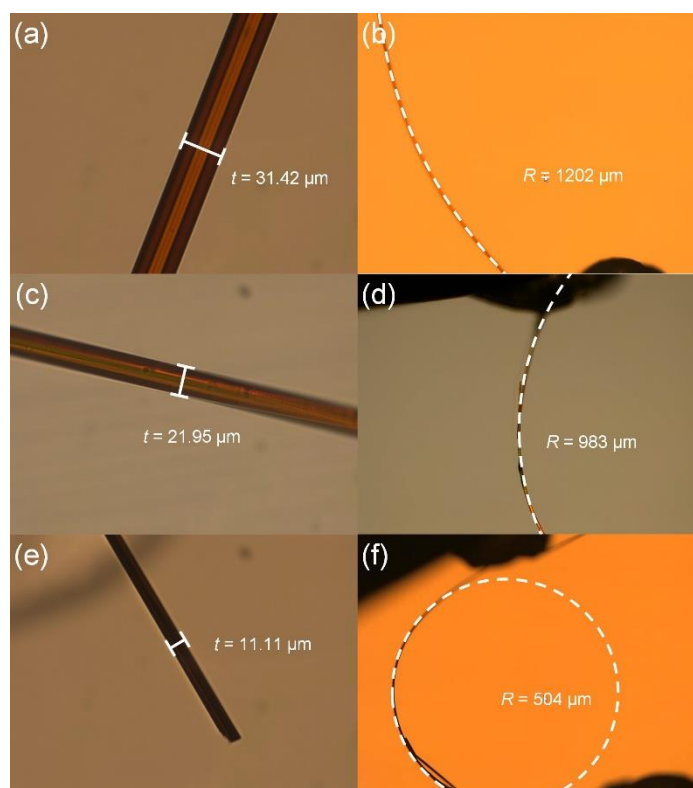


**Fig. S3.** Strain measurement for crystals of **2**.

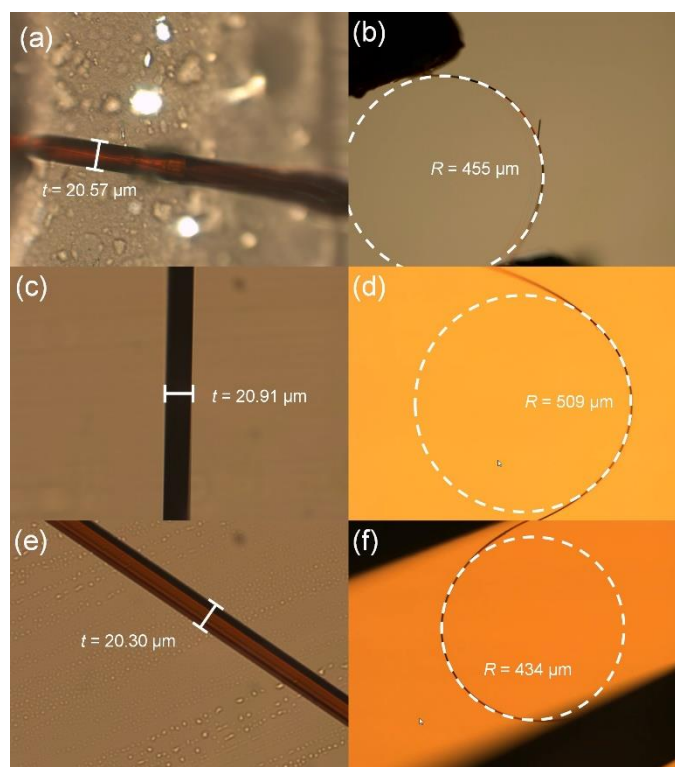


**Fig. S4.** Strain measurement for crystals of **3**.

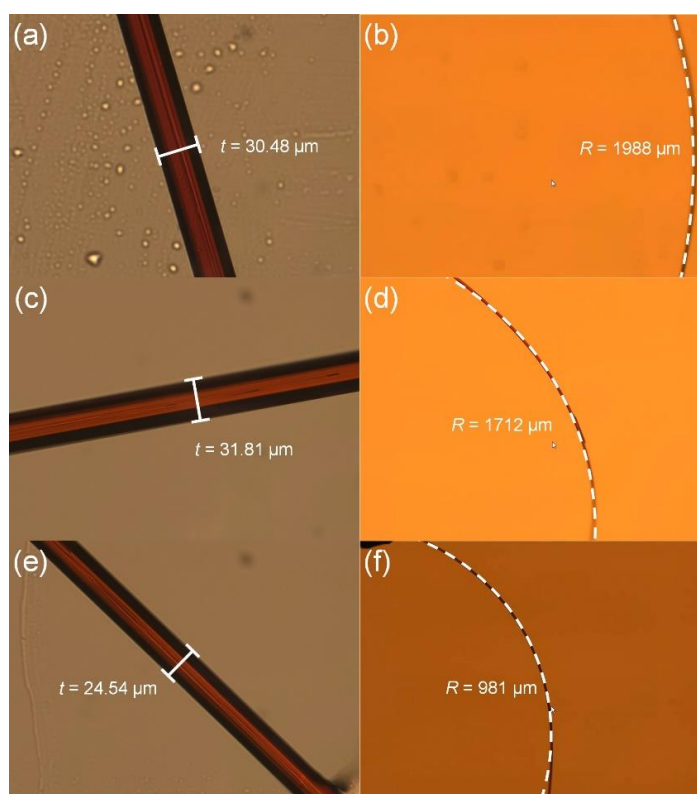


**Fig. S5.** Strain measurement for crystals of **4**.

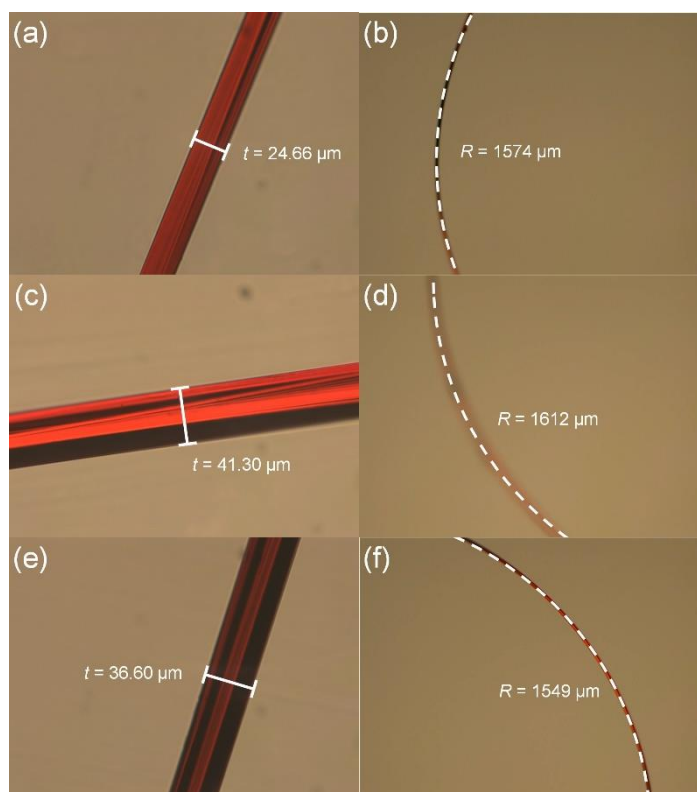


**Fig. S6.** Strain measurement for crystals of **5**.

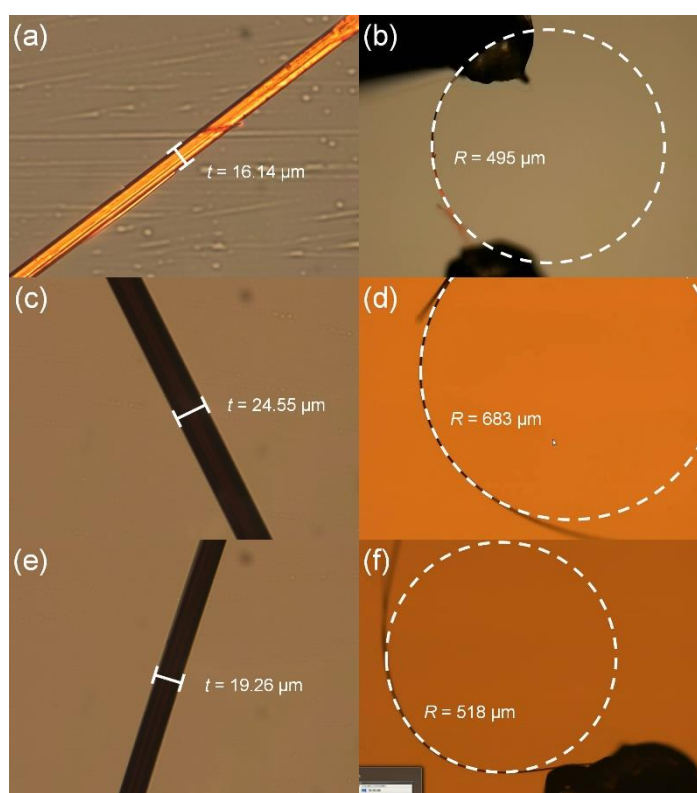


**Fig. S7.** Strain measurement for crystals of **6**.

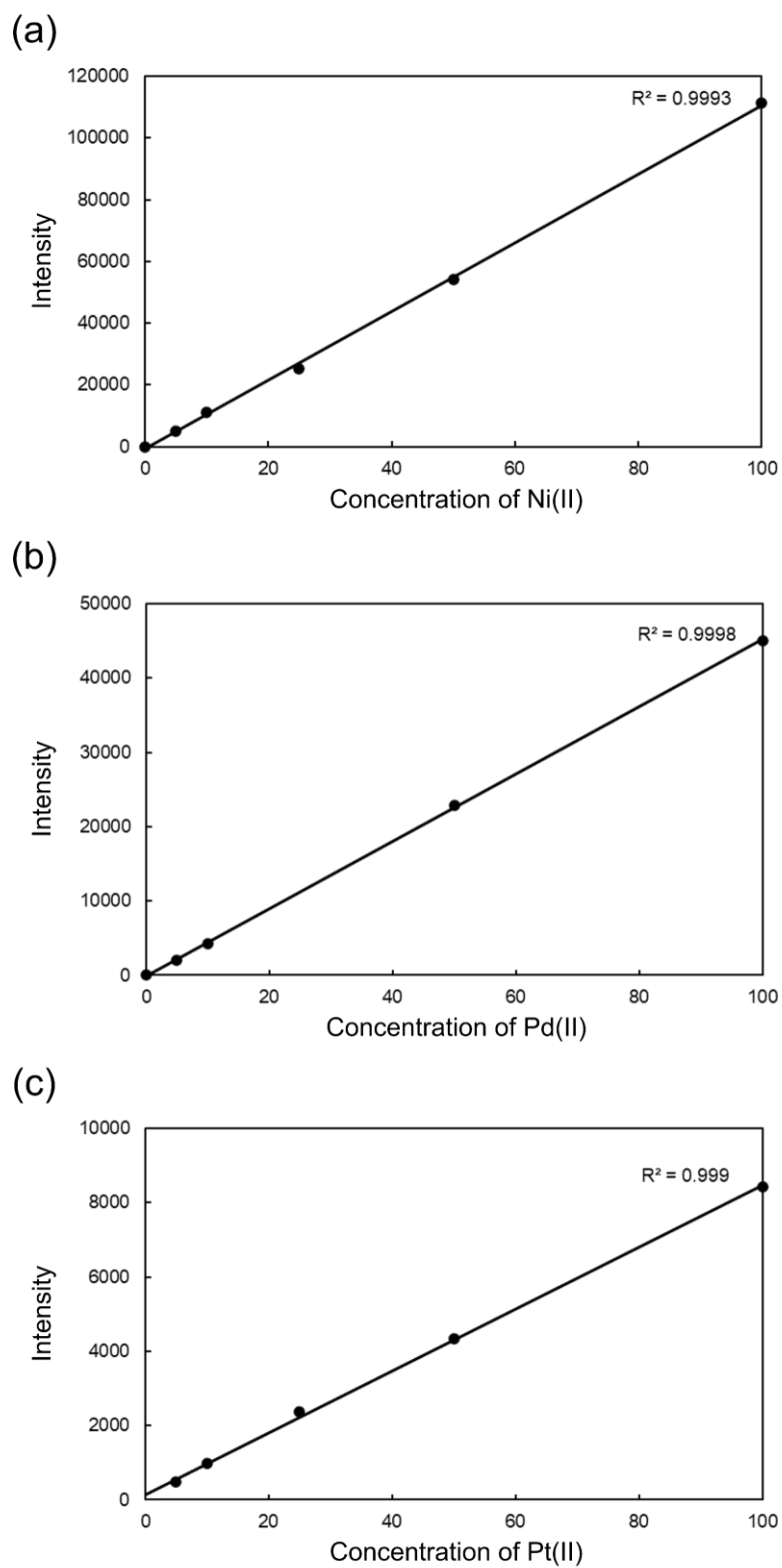


**Fig. S8.** Calibration curves for (a) Ni(II), (b) Pd(II), (c) Pt(II) for ICP-OES measurements.



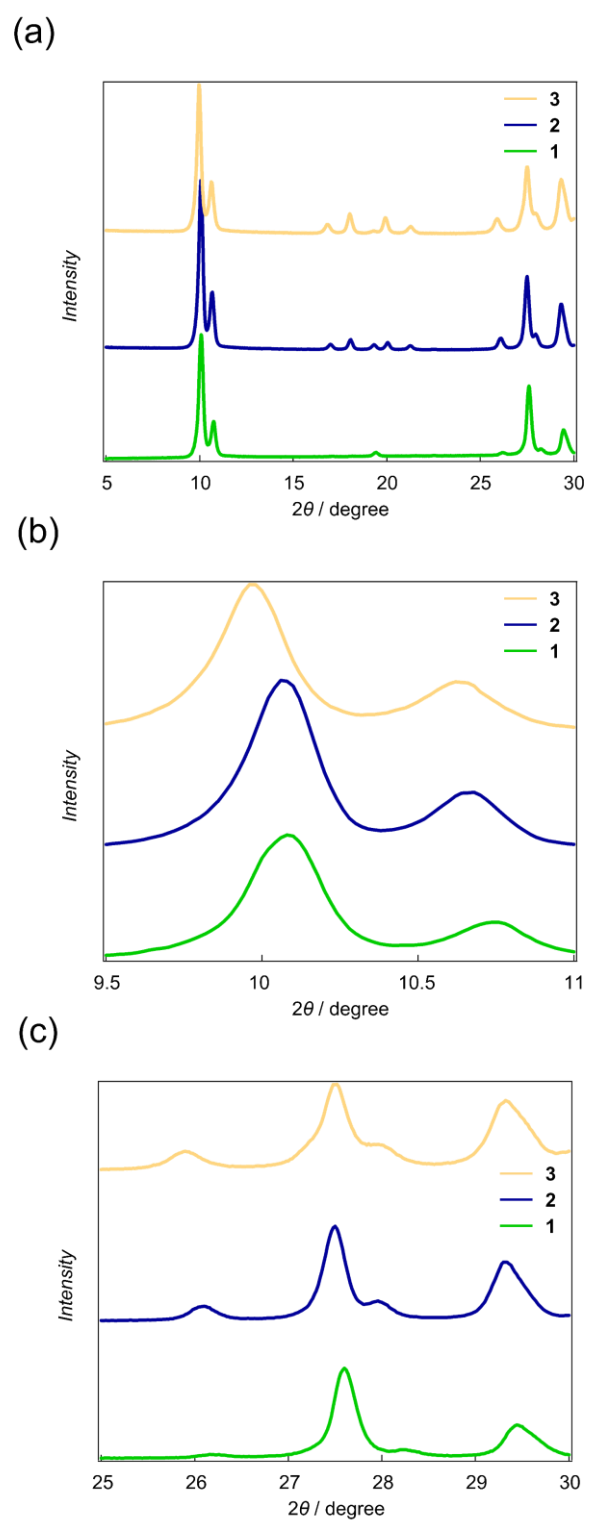


**Fig. S9.** PXR D patterns for 1–3.

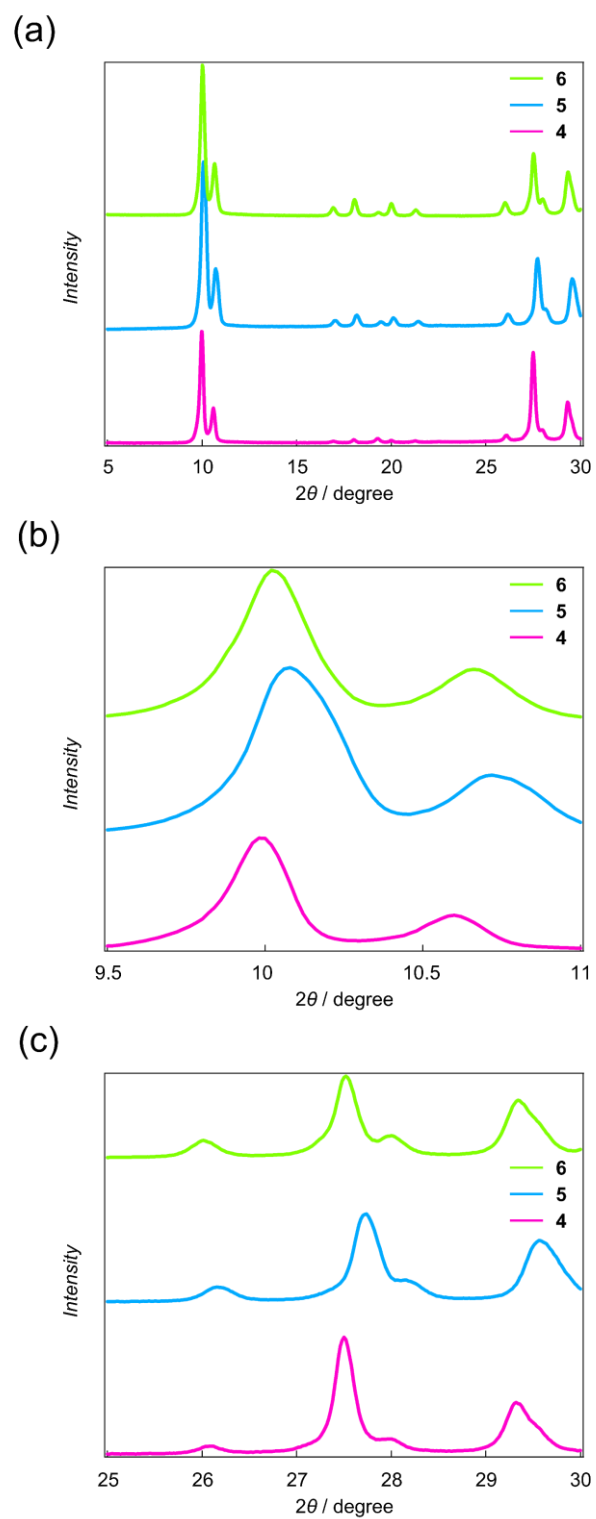
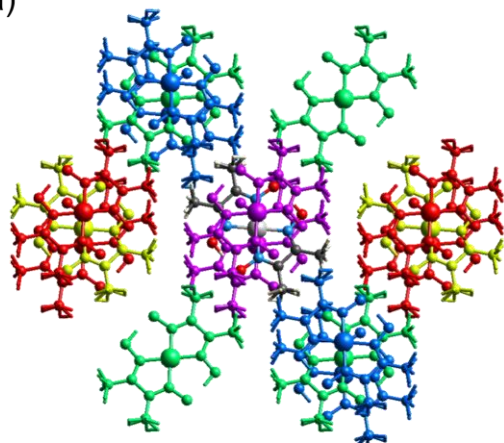


**Fig. S10.** PXR D patterns for 4–6.

## Energy framework calculations

(a)

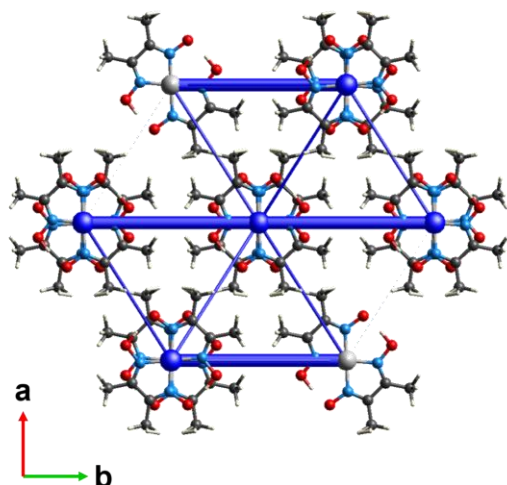


Interaction Energies (kJ/mol)  
R is the distance between molecular centroids (mean atomic position) in Å.

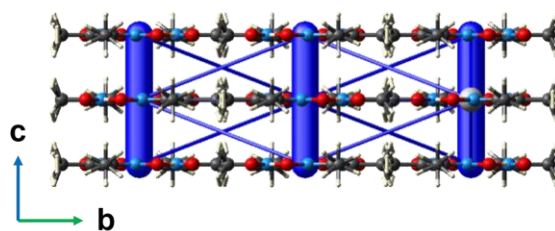
Total energies, only reported for two benchmarked energy models, are the sum of the four energy components, scaled appropriately (see the scale factor table below)

	N	Symp	R	Electron Density	E <sub>ele</sub>	E <sub>pol</sub>	E <sub>dis</sub>	E <sub>rep</sub>	E <sub>tot</sub>
	4	x, -y, -z+1/2	10.95	HF/3-21G	-2.6	-6.2	-7.6	4.4	-9.9
	2	x, y, z	10.47	HF/3-21G	-35.4	-9.4	-9.5	3.0	-48.3
	4	x+1/2, -y+1/2, -z	9.76	HF/3-21G	-2.7	-16.2	-22.9	41.6	-0.2
	4	x+1/2, y+1/2, z+1/2	10.27	HF/3-21G	-28.7	-13.2	-26.8	62.1	-11.6
	2	x, -y, -z+1/2	3.21	HF/3-21G	-22.5	-86.0	-125.9	131.9	-85.4

(b)



(c)



Energy frameworks were constructed from pairwise intermolecular interaction energy calculations (for crystal geometry) using the HF/3-21G molecular wave functions in CrystalExplorer17.5 [Reference 12a in the main manuscript). The calculated total interaction energy contains electrostatic, polarization, dispersion and exchange-repulsion terms.

**Fig. S11.** (a) Output of total interaction energy decomposition. (b) Energy frameworks for **1** in total interaction strengths viewed down the *c*-axis and (c) viewed down the *a*-axis. (b) and (c) were displayed in Fig.4.

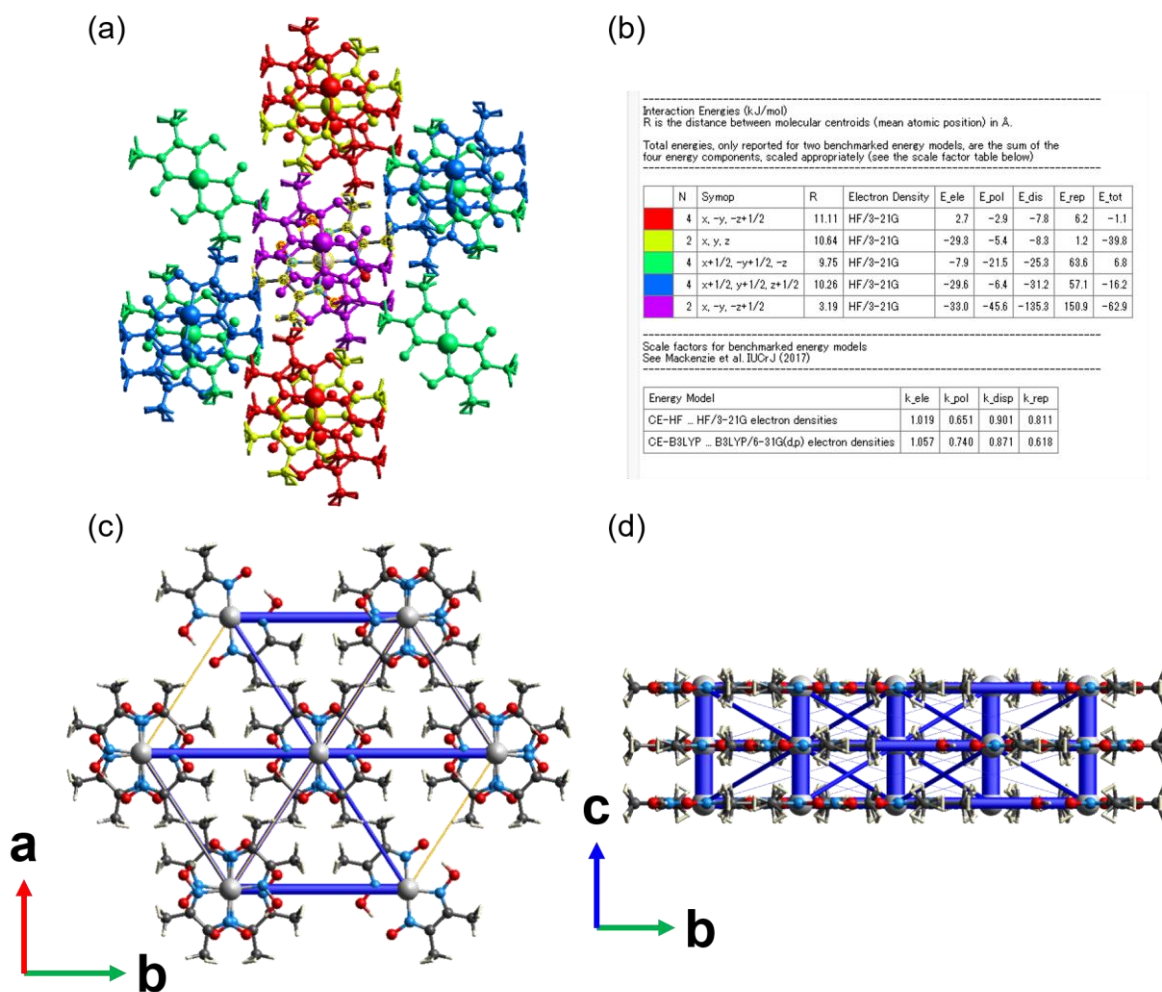


**Fig. S12.** (a) Output of total interaction energy decomposition. (b) Energy frameworks for **2** with total interaction strengths viewed down the *c*-axis and (c) viewed down the *a*-axis.

**References**

- [1] Y. Y. Titova, L. B. Belykh and F. K. Shmidt, *Russ. J. Gen. Chem.*, 2014, **84**, 2413-2420.
- [2] T. Kamata, T. Kodzasa, H. Ushijima, K. Yamamoto, T. Ohta and S. Roth, *Chem. Mater.*, 2000, **12**, 940–945.
- [3] Cs. Várhelyi, A. Kovács, Á. Gömöry, Cs. Várhelyi, Gy. Pokol, Gy. Farkas and P. Sohár, *J. Coord. Chem.*, 2009, **62**, 2429–2437.
- [4] M. Đaković, M. Borovina, M. Pisačić, C. B. Aakeröy, Ž. Soldin, B.-M. Kukovec and I. Kodrin, *Angew. Chem. Int. Ed.*, 2018, **57**, 14801–14805.